Proceedings of the Seventh International Conference on
Railway Technology: Research, Development and Maintenance
Edited by: J. Pombo
Civil-Comp Conferences, Volume 15, Paper 3.16
Civil-Comp Press, Edinburgh, United Kingdom, 2026
ISSN: 2753-3239, doi: 10.4203/ccc.15.3.16

NTSB Investigations of Vertical Split Rim Failures of Freight Train Wheels

E. M. Mueller[1] and X. Liu[2]

[1]Office of Research and Engineering, National Transportation Safety Board (NTSB), Washington, DC, United States of America
[2]Meta, Seattle, WA, United States of America

Abstract

Freight rail accidents can release volatile petroleum products, with serious and even fatal consequences. One of the leading types of railroad wheel failures observed in North America is vertical split rim (VSR) cracking — a rapid, unstable propagation of a subsurface cracks that develop parallel to the front rim face. The National Transportation Safety Board (NTSB) investigates freight derailments carrying hazardous materials in the United States. One of the first investigations into wheel failures from a VSR resulted in several recommendations for prevention and mitigation. Unlike shattered rims and thermal cracks, VSRs require continuous monitoring of impact loads to assess their progression. The NTSB Materials Laboratory employed multiple characterization techniques, including electron microscopy, x-ray diffraction for residual-stress mapping, hardness mapping, and modelling to determine areas of stress concentration. The materials examination helped determine the probable cause of the derailment, and the results of this investigation led to changes in freight rail operations in the US and Canada.

Keywords: vertical split rim, failure analysis, residual stress, wheel impact load detector, accident investigation, wheel, wheel-rail interaction

1 Introduction

The National Transportation Safety Board (NTSB) is an independent United States federal agency charged with determining the probable cause of transportation accidents, promoting transportation safety, and assisting victims and their families.

This investigation mandate includes freight rail accidents, including derailments from wheel fractures. While shattered rim defects were once more common, vertical split rim (VSR) fractures have become a predominant mode of wheel failure.

Vertical split rims are a type of progressive wheel failure brought on by developing internal residual stresses [1]. VSRs are common in the western United States and Canada, mainly in AAR Class-C rim-quenched wheels [2]. In contrast, shattered rim wheel fractures were once common, but advances in manufacturing reduced the inclusions and pores that caused this failure mechanism [3]. In the United States and Canada, where the rail network is dominated by long freight consists, vertical split rim (VSR) fractures persisted as a major wheel failure mode [4]. Improvements in wheel manufacturing were ineffective in reducing this type of failure [5].

Other conditions associated with VSR failures include high-impact loads, thin rim thicknesses, and a statistical increase during winter months [6]. While not singularly conclusive, studies of vertical split rim failures point to heavy loading and long service times as common factors. While other countries have definite life-limits for freight wheels under the heaviest allowed loads, in the US, freight wheels are allowed to remain in service until they reach industry-condemning limits. These wheels often accumulate high service miles with small tread shells and small, shallow rim cracks [1].

On May 6, 2015, a BNSF crude oil unit train, U-TIOCXP0-44T, derailed near Heimdal, ND. The weather at the time of the accident was 14 °C with overcast skies. At the scene of the derailment, witness marks were present on the rail every 2.89 meters leading up to the point of derailment. Two pieces of broken wheel were found along with the wheel remnant and axle that were part of tank car TRFX 1224. The fractured wheel fragments, sectioned axle halves, and intact wheel were sent to the NTSB Materials Laboratory in Washington, D.C., for testing and failure analysis. The Materials Laboratory determined that the wheel fractured from a vertical split rim mechanism. This and other findings helped develop recommendations to prevent this fracture mode from recurring.

2 Methods and Materials

The wheel had been manufactured by Griffith Wheel Company in Keokuk, IA, USA, per the 2011 version of the American Association of Railroads (AAR) M-107 Class C specification [2]. The wheel was cast to the CH-36 size standard (36-inch or 91.4 cm diameter), but the date could not be determined due to damage to the wheel surfaces. The wheel was examined at the NTSB Materials Laboratory in Washington, DC, USA. The parts were photographed using a Canon EOS Rebel T3i digital camera and Keyence VHX-1000 digital microscopes. The digital microscopes produced high dynamic range and composite high depth-of-field images.

Specimens excised from the fractured wheel were examined using a Zeiss Auriga 40 field emission scanning electron microscope (SEM). This microscope was equipped with a Thermo Scientific UltraDry NORAN System 7 energy-dispersive X-ray spectroscopy (EDS). Specimens were cleaned sequentially in an ultrasonic bath with an aqueous powdered detergent solution and a chelating rust-removing solution. Several metallographic cross-section specimens of the forward and aft propeller welds were mounted, polished to 0.05 µm grit, and etched using a 2% Nital solution. These specimens were inspected using a Zeiss Axio Observer *Z1*m inverted microscope for metallography.

A radial section was macroetched using a solution of hydrochloric acid (HCl), sulfuric acid (H_2SO_4), and water at 71 °C. Hardness testing was performed per ASTM E10 and ASTM E18 for the Brinell and Rockwell scales, and the data were compared with the requirements for AAR-M107 Class C wheels [2]. Microindentation hardness mapping was performed using a LECO AMH-43 automated hardness tester, per ASTM E384.

Specimens from the fractured wheel were cross-sectioned and examined by X-ray diffraction (XRD) at Lambda Tech, Cincinnati, OH, USA, to determine subsurface residual stresses. The XRD measurements were made at 0.2-inch intervals from the tread surface towards the interior in the axial, radial, and 45° directions, performed per SAE HS-784 using the (211) planes.

The sections near and around the fracture surface were scanned using a FARO Quantum portable measurement probe with a FARO Laser ScanArm laser scanner. The data were rendered and converted to point clouds and wire meshes using Geomagic Studio 12.0.0. A 3D finite element model of the accident train axle assembly was constructed using Abaqus 6.14-1.

3 Results

The fractured wheel fragments are shown in Figure 1, as found on-scene. This wheel exhibited four fractures towards the outer tread surface that were generally radial in orientation. There was also a slanted fracture closer to the axle location, oriented parallel to the circumferential direction of the wheel. This inner circumferential fracture mirrored that of the remnant still attached to one of the axle sections. Ultrasonic nondestructive inspection did not reveal any internal indications consistent with voids, inclusions, or discontinuities.

The second largest fragment of the fractured wheel exhibited a vertically oriented fracture surface on the outboard-facing rim of the wheel. This fracture is illustrated in Figure 2. This fracture exhibited three regions: an outer and an inner region, each oriented parallel to the running circumference of the train wheel, and a middle vertical region, oriented perpendicular to the wheel circumference.

Figure 1: Fractured wheel remnants, photographed at the accident site.

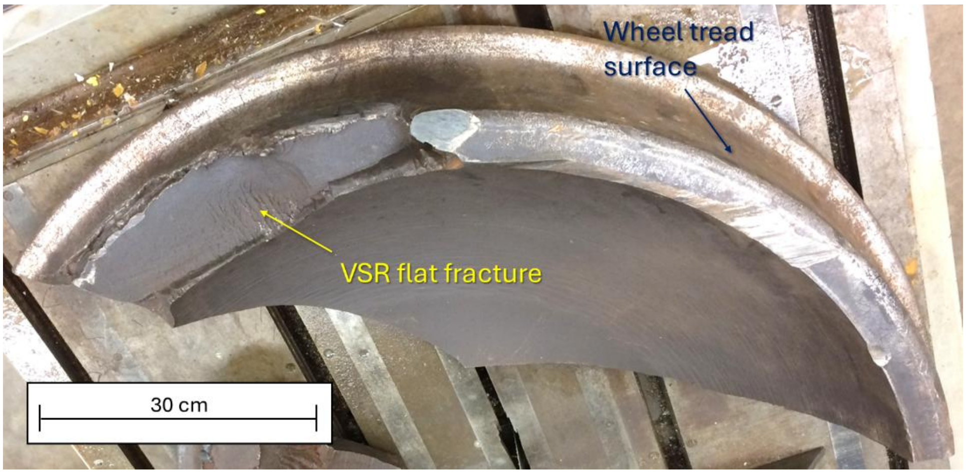

Figure 2: Wheel fragment with the flat vertical fracture face, as received.

3.1 Destructive Testing and Visual Examination
The fractured train wheel fragment with the vertical fracture face was sectioned repeatedly to produce specimens for additional testing and examination. Figure 3 shows the initial sections of this train wheel segment, the label given to each section in this study, and the purpose of several of the pieces.

Figure 4 shows the tread surface of the wheel facing the reader, after cleaning. This tread surface exhibited heavy batter and deformation adjacent to the fracture, consistent with heavy impact forces and spalling of the thread surface and outer wheel. The initial fracture region displayed crack arrest marks, consistent with fatigue crack propagation, present approximately 33 mm below the wheel tread surface. These arrest marks were oriented parallel to the tread running surface, propagating from the rim to the inner flange of the wheel.

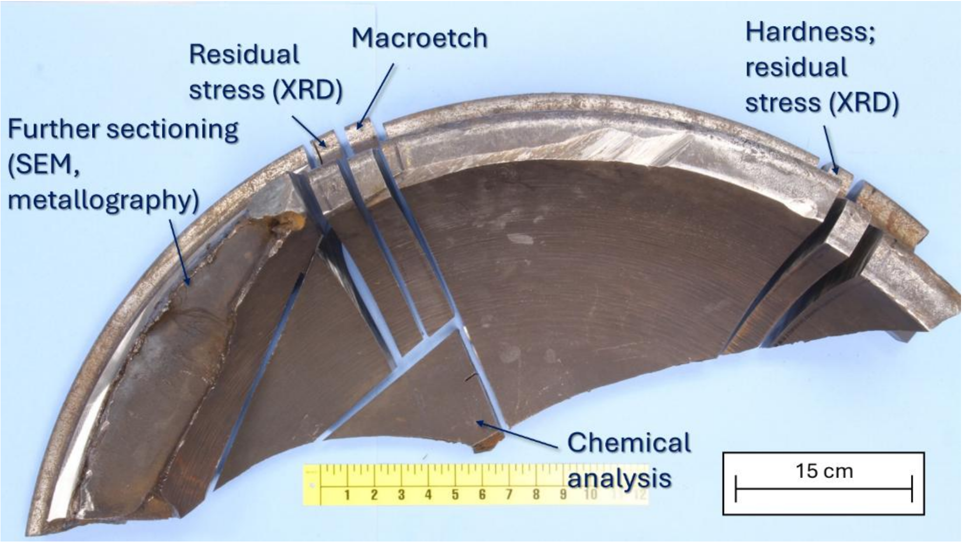

Figure 3: Sections of the VSR wheel remnant and their respective testing purposes.

Figure 4: The subsurface (initial) progressive cracking viewed from the tread surface

Using digital calipers, these progressive cracks were approximately 15 mm in length from the vertical fracture face until they ran under the battered tread surface of the wheel. The presence of ratchet marks between the cracks was consistent with multiple cracks initiating separately and coalescing as they propagated. The vertical fracture face was oriented flat, exhibiting a rougher texture than the progressive fracture described above. The vertical fracture face exhibited river patterns consistent with the fracture growing from near the wheel tread toward the interior. No indications of progressive fracture were present on this section of the fracture surface.

Figure 5 shows the inner set of visible crack arrest marks, consistent with fatigue propagation from the vertical fracture face towards the rim (field side) of the wheel. The largest portion of this progressive fracture extended approximately 38 mm away from the vertical fracture face.

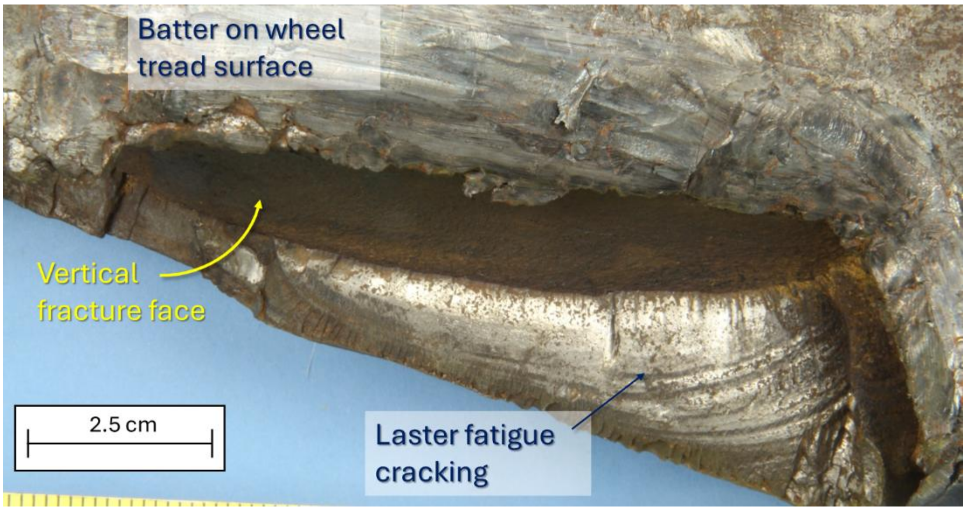

Figure 5: Surface batter on the wheel tread surface, the vertical fracture face, and the inner perpendicular progressive fracture

The macroetched section is shown in Figure 6. The wheel cross-section exhibited the dendritic structure typical of cast train wheels. No porosity or inclusions were noted on this sample. This etchant produced a darker contrast along the running surfaces, as annotated in the figure. Later optical metallographic examination showed a core microstructure of fine pearlite within the starburst morphology. The microstructure of the wheel closer to the surface also displayed a fine pearlite microstructure; however, the features were flattened and smaller, consistent with deformation present towards the wheel contact surface.

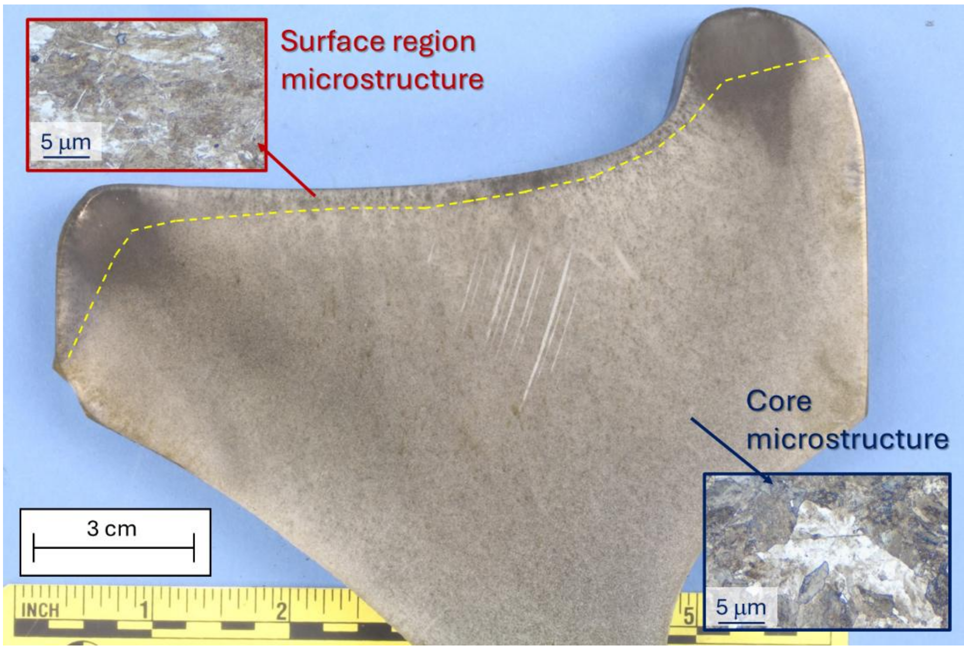

Figure 6: The macroetched cross section through intact wheel regions, showing different microstructure superimposed, and the area of surface distress annotated.

3.2 Scanning Electron Microscopy

The subsurface cracking oriented parallel to the wheel tread surface exhibited striations consistent with fatigue crack propagation. No indications of other progressive cracking mechanisms were observed. Likewise, the vertical subsurface cracking was consistent with fatigue. The nature of the fatigue striations was consistent with the crack propagating from inside out towards the tread surface.

Examination of the larger vertical fracture face revealed a slanted dimple rupture, consistent with overstress failure. Examination of the lower/inside progressive fracture shows fatigue striations. The striations propagated from the vertical overstress fracture towards the rim of the wheel.

3.3 Optical Metallography and Microindentation Hardness Mapping

Figure 7 shows a montage of the tread surface cross-section The fatigue fracture surfaces were oriented towards the left, with the top of the vertical overstress region in the lower left, with the tread surface facing upward. There was a large crack extending from the fatigue fracture parallel to the tread surface. This orientation and the features of this crack were consistent with the fatigue crack pictured in Figure 4 running from right to left. There was also an internal crack perpendicular to that crack, which extended towards the tread surface. At the terminus of the large crack parallel to the tread surface, the crack appeared to turn toward the wheel surface.

There were also cracks at the tread surface consistent with propagation from the outer surface inward (top of Figure 7). The surface material was white in color with no internal features, consistent with untempered martensite that formed when the steel was exposed to high temperatures and rapidly cooled as the heat dissipated into the bulk of the wheel [7]. Cracks were present between this surface phase and extended into the bulk of the wheel material.

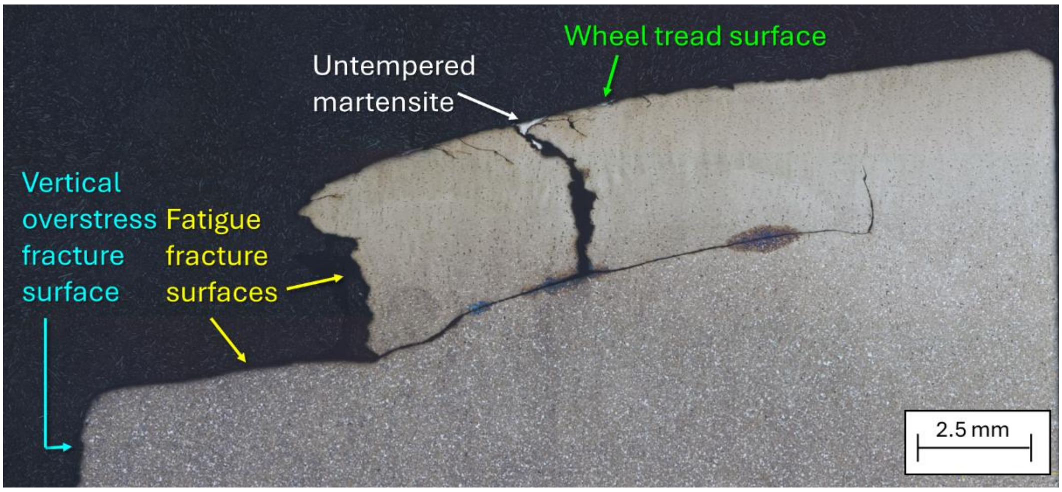

Figure 7: Cross-section through the fracture surface, showing subsurface cracking, as well as the location of the fracture surface features.

The tread surface of the wheel also exhibited high deformation and distress near the contact surface and at fracture surfaces. The grain flow lines bent toward the fracture surfaces, consistent with the batter and material flow viewed on the tread surface. Cracks were present in and through these highly deformed areas.

Figure 8 shows the data compiled as a false-color map, with hardness values organized from softest (yellow/green) to hardest (purple/red). The material closest to the train tread surface exhibited a higher hardness, up to 45 HRC (452 HV500), than the interior material, ~36 HRC (354 HV500). Along the crack (oriented horizontally), the difference in hardness was the highest between the outer and inner regions. This higher hardness near the tread surface was consistent with higher deformation and cold working present in the area.

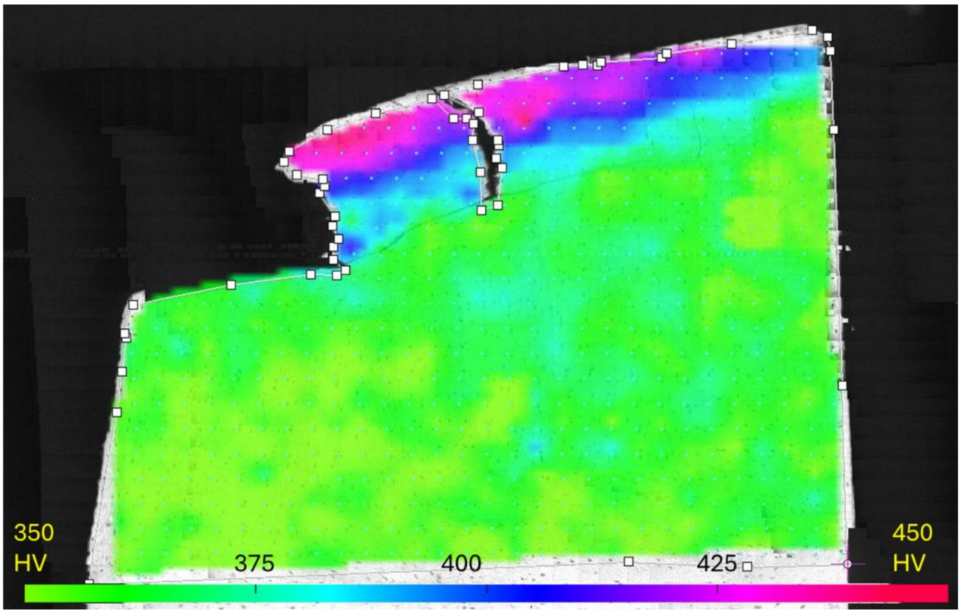

Figure 8: – False colored hardness map of a wheel cross-section showing color from softest material (green) to hardest material (purple/red) in HV_{500}.

3.4 XRD Results

Two wheel cross sections were examined with XRD measurements made at nominal distances approximately 5 mm apart from the tread surface towards the interior at axial, radial, and 45° directions. The XRD measurements were performed per SAE HS-784 using the (211) planes of the nominal body-centered cubic (BCC) steel structure.

The XRD analysis revealed tensile and compressive residual stresses in the wheel cross-section. Towards the surface, a compressive residual stress was measured with a maximum of -294 MPa (-42.6 ksi) in the axial direction. This residual stress inverted at approximately 5 to 15 mm below the wheel tread surface, producing an internal tensile residual stress. The maximum tensile residual stress was +441 MPa (+64.0 ksi) in the radial direction.

3.5 Other Testing

Cross sections of the wheel were taken and ground to facilitate Brinell hardness testing and Rockwell hardness testing per AAR M-107, Section 11.5. The wheel rim hardness was also measured after sectioning and grinding, as in Section 10.1. The rim hardness averaged 341 HBW, meeting the Class C wheel requirement (321-363 HB). The cross-section Brinell hardness ranged from 331-361 HB, within the required range of 301-363 HB for Class C wheels. The Rockwell hardness data were all within the Class C wheel tolerance of 30-42 HRC.

Chemical composition testing, performed both by the NTSB Materials Lab and by an external laboratory, was consistent with the requirements for AAR M-107 Class C wheels.

Laser-scanned data from the fractured wheel were integrated with the loading profile of a standard CH-36 wheel. When modelled with the lateral and bearing loads on the tread surface, the residual stresses in the subsurface tensile zone were found to exceed the yield stress of the Class C wheel material. This model suggested that any crack that grew deep enough could split the wheel rim due to the large residual tensile stresses.

4 Analysis and Discussion

In this accident, the train derailed due to a wheel fracture caused by a vertical split rim failure. The fracture morphology, microscopic fracture features, direction of the secondary cracks, local microstructural changes, and inversion of residual stresses were all consistent with the observed vertical split rim fracture sequence [6].

The distribution of internal residual stresses drives the development of vertical split rim failures. For cast wheels after manufacture, the wheels generally exhibit a neutral residual stress profile, exhibiting some compressive residual stress caused by the rim quenching operation.

While often beneficial when designed for, compressive residual stresses that accumulate in service can cause rapidly progressing internal cracks in freight wheels. As wheels accrue service hours, surface damage imparts a region of higher axial compressive stress along the tread surface. This layer must be balanced internally, thus creating a corresponding region of internal axial tensile stress. This residual tensile stress zone, peaking about 1.3 cm below the tread surface, was found to develop over long service times in class C wheels [1].

A study proposed the following steps in the failure of a wheel due to VSR [8]:

- Tread damage from surface shelling or spalling creates fatigue cracks that propagate under service loads.
- Crack propagation into an internal zone of residual tensile stress leads to rapid downward vertical crack growth.

- Subsequent service loads, such as rolling contact, bending moments, and pounding from impacts, eventually lead to complete wheel failure.

Tread damage from shelling and spalling is the primary contributor to initiating vertical split rim failures. Fatigue cracks initiate from these defects and propagate into the rim section under service loads. Once a crack initiates in the surface layer, it propagates at a shallow angle down into the wheel and back up to the tread, typically resulting in the detachment of a small piece of tread material, referred to as a shell [9]. Service conditions with rolling-contact fatigue are detrimental to wheel service lives [10].

In this accident, the locations of different fracture regions corresponded to the changes in residual stresses measured by XRD. The fatigue cracks, generally oriented parallel to the tread surface, were consistent with the areas of compressive residual stresses. Conversely, the areas with the measured residual tensile stress were consistent with the location of the perpendicular vertical transgranular overstress crack propagation [11]. This residual stress profile was consistent with those observed in vertical split rim failures [3]. When cracks from tread surface damage propagated into this sub-surface axial tensile zone, the crack turned and rapidly accelerated until the tensile stresses were relieved.

Loaded tank cars typically weigh 286,000 pounds (129,727 kg) and carry some of the heaviest loads impacting the railroad infrastructure. During this investigation, the Transportation Technology Center (TTC), operated by the consortium ENSCO on behalf of the US Department of Transportation, tested train wheels under both laboratory and field conditions, including finite element modelling. Crack-propagation studies used induced flaws to examine the effects of crack growth rate, wheel and rail loads, and ambient temperature [8-9]. In a study conducted by the TCC (then the Transportation Technology Center, Inc. or TTCI) involving 24 wheel sets with broken wheels, the dominant failure mode (71%) was VSR. In six of the 12 broken wheels for which historical data were available, impact loads exceeding 90 kips (400 kN or 40.8 metric tons) were reported before failure [12].

Research into the effects of accumulated mileage and high temperatures on axial residual wheel stresses has shown that residual stresses develop in the wheel rim within the first few thousand miles of service. Elevated wheel temperatures from prolonged braking alter the residual stress pattern by shifting the internal residual tensile stress region closer to the surface [13]. Recreating a VSR defect under test conditions has been found difficult, yielding inconclusive results [14]. Wheels without defects have been found to fail quickly, and wheels with induced defects have been tested without VSR development. However, recent testing with drop hammers used to recreate accumulated residual stresses has shown good correlation with finite element modelling in wheel tests simulating VSRs [15].

Train wheels also develop localized microstructural changes from wheel tread burning. This process forms brittle martensite at the surface, becoming a greater influence than the rolling-sliding wear on the tread surface [16]. Cracks initiate at and propagate along the plastic deformation line, and the extent and severity of fatigue damage positively correlate with the material's carbon content [17]. Steels with lower carbon content and bainitic microstructures may outperform pearlitic steels because their lower hardenability reduces the likelihood of martensite formation. If martensite forms, it is generally less brittle due to its lower carbon concentration and higher MS temperature [7]. However, while decreasing carbon content can increase fatigue resistance, the surface wear resistance decreases [18]. The fractured wheel in this investigation exhibited cracking collocated with surface martensite.

Wheel impact load detectors, or WILDs, are electronic data-collection devices that measure the vertical impact forces of wheels on rail using rail-mounted strain gauges placed on the rail web. A WILD can measure impact forces caused by flat, shelled, spalled, out-of-round, and damaged wheels, as well as by wheels with built-up tread. In North America, the data are measured in kips, or 1000 lbs. of force (4.45 kN or 0.45 tonf). High-impact wheel forces can damage cargo and track infrastructure, primarily rails. Severe stress on a wheel from impacting the rail can cause a fracture that spreads and starts chipping off pieces of the tread surface. Examination of the WILD data from this car (TRFX 1224) found the average load increased from November 2014 to May 2015, with four instances of readings at or above 80 kips (356 kN) [19].

The Federal Railroad Administration, an agency of the US Department of Transportation, based on its safety advisory and the accident WILD data, enforces rail safety regulations. While they had promulgated a safety advisory on high-impact loads, the railroads failed to adopt it universally. As high-hazardous freight trains (HHFT), like those carrying only crude oil in this case, present an extraordinarily high risk to the public, it is recommended that the FRA and the AAR evaluate what impact load thresholds are safe, and then revise the FRA safety advisory and the AAR interchange rules.

Specific data on VSR failures in the United States are limited because most train wheel fractures have been categorized as shattered rims, which are typically caused during manufacturing. The Transportation Safety Board of Canada (TSB) has investigated accidents where a VSR was the probable cause. In the three most prominent investigations at the time, cars had received exceeding 80 kips (356 kN) in the months before the wheel failure from VSRs [20].

According to the rail company, BNSF, they had not changed their handling instructions for wheels reading 60-, 70-, and 80-kips (or 267, 311, 356 kN). BNSF raised the profile of alerts by: (1) replacing car wheels with readings greater than or equal to 80 kips (356 kN) while on the repair tracks, and (2) replacing car wheels with 90 kips (400 kN) or more in the train yard. In September 2016, only two of the eight freight and passenger railroads had adopted elements of the FRA's safety advisory, with two having restrictions that exceeded the AAR requirement for 80 kips or more (356 kN).

New technologies, such as on-board detectors, plastic strain evaluation, and digital twins, may all improve the accuracy of wheel damage detection [21-22]. However, interpreting the immense amounts of wayside and on-board data will be required to make accurate, timely life-limiting predictions for wheels [22]. Integrated systems based on validated simulations of worn wheel profiles show promise, though examining the influence of other inputs (such as braking) will be needed [23].

4 Conclusions and Contributions

A BNSF crude oil train, U-TIOCXP0-44T, derailed near Heimdal, ND. The NTSB determined that the probable cause of this derailment was the failure of a wheel on the 81st tank car due to a vertical split rim. The fractured wheel exhibited subsurface fatigue cracking parallel to the tread surface, followed by a vertical overstress fracture perpendicular to the tread surface, running inward. The later fatigue crack propagation of the split wheel under repeated service loads led to catastrophic failure of the wheel.

Vertical split rim failures are statistically more common in North America than in other parts of the world. The common use of train wheels under heavy loads and long service life can create surface residual compressive stress zones, which are balanced by a sub-surface residual tensile stress zone. In this case, the wheel's accumulated subsurface residual stress zones led to VSR failure.

Following this accident, the NTSB recommended that the FRA evaluate wheel impact load thresholds most likely to lead to VSR failures, particularly on HHFTs. In addition, the NTSB recommended that the FRA and AAR collaborate to determine safe load thresholds and revise the interchange rules to reflect these changes. The AAR countered that wheel impact loads alone were not a reliable enough method to detect imminent wheel failures, but that high load readings and thinning wheel rims used together could predict broken wheels. In January 2016, the AAR amended its rules to remove wheels with a dynamic load of 222 kN (50 kips) or more combined with a rim thickness of less than 2.54 cm (1 inch). The FRA also performed studies on VSR failures [1] and began classifying VSR wheel failures as separate defect codes in 2018.

Since this accident, another major derailment, hazardous material release, and fire occurred in East Palestine, Ohio, USA, on February 3, 2023. This derailment was caused by a bearing that overheated, failed, and led to an axle separation [24]. One of the issues was the inability of the wayside bearing and wheel load detector systems to detect a problem with the consist. At the time of this writing, multiple recommendations to the regulator and trade associations governing freight rail transport are open. However, the agency has noted the lack of industry consensus on minimum standards for wayside systems, including alert and alarm thresholds and operating rules. The effectiveness of wayside bearing defect detection systems depends on appropriate operational responses. Because the rail industry has yet to reach consensus on a standard for these responses, research is needed to determine which operational responses to bearing alerts and alarms are sufficient to prevent bearing-related accidents.

Acknowledgements

In accordance with Title 5 Code of Federal Regulations §2635.807(b)(2), the views expressed in this article are those of the authors and do not represent the views of the National Transportation Safety Board or the USA. The authors would like to thank NTSB investigators Jim Southworth and Joey Rhine for their help with these investigations.

References

[1] Jones, K., Cummings, S., Tournay, H. "Vertical Split Rim: Causes and Prevention." FRA Technical Report. DOT/FRA/ORD-23/30. Washington, DC, USA (2023)

[2] AAR M-107 – *Manual of Standards and Recommended Practices, Wheels, Carbon Steel* (2011 revision), American Association of Railroads, Washington, DC.

[3] S. Kalay, D. Stone, and C. Lonsdale, Transportation Technology Center, Inc., *Effect of Wheel Impact Loading on Shattered Rims* (2001).

[4] Broken Rims in Railroad Wheels: DOT/FRA/ORD-14/41 Final Report. Federal Railroad Administration (2014).

[5] S. Kalay, D. Stone, and C. Lonsdale, Transportation Technology Center, Inc., *Effect of Wheel Impact Loading on Shattered Rims* (2001).

[6] Lonsdale, C., Oliver, J., Maram, R., & Cummings, S. (October 2013). Development of Railroad Wheel Rim Axial Residual Stress in Heavy Axle Load Service (Paper RTDF2013-4716). In *Proceedings of ASME Conference*. American Society of Mechanical Engineers, New York, NY.

[7] H.K.D.H. Bhadeshia, "Modern Bainitic Steels," *Bainite in Steels: Transformations, Microstructure and Properties, 2nd Edition*. London: The Institute of Metals, (2001) p. 387

[8] C. Lonsdale, J. Oliver, "North American railways combat split wheel rims," *International Railway Journal*. (2014)

[9] A. Ekberg, E. Kabo and H. Andersson, "An Engineering Model for Prediction of Rolling Contact Fatigue of Railway Wheels," *Fatigue and Fracture of Engineering Materials and Structures*, 25 [10], October 2002

[10] N.F. Strey, A.B. Rezende, R. da Silva Miranda, S.T. da Fonseca, R.B. Mei, C. Scandian. "Comparison of rolling contact fatigue damage between railway wheels and twin-disc test specimens. *Tribology International*. 160. (2021) 107037.

[11] S. Cummings, "Strategies to Prevent Wheel Failures." *18th Annual AAR Research Review*. (2013) pp. 12-15

[12] TTCI. "Broken Wheel Inpsections." Technology Digest TD-09-008. (2009)
[13] "Development of Railroad Wheel Rim Axial Residual Stress in Heavy Axle Load Service" by Cameron Lonsdale, et al., proceedings of the ASME Rail Transportation Division 2013 Fall Technical Conference.
[14] K. Jones, S. Cummings. "Wheel Failures: Digging Down to the Roots," *RailwayAge* (September 10, 2014).
[15] C. Lonsdale, T. Rusin, T. Hay. "Research to Understand the Effects of Wheel Impact Loads on Wheel Stress Levels." *Proceedings of the 2009 ASME Joint Rail Conference*. JRC2009. March 3-5, 2009, Pueblo, CO, USA
[16] K.J. Sawley, J.A. Benyon, E.G. Jones, *9th International Wheelset Congress*, Quebec, QC, Paper 2-6 (September 1988) pp. 1-12.
[17] P. Laczko, P.J. Mutton. "Metallurgical and NDT Aspects in the Management of Overheated Railway Wheels." *Materials Forum*. 30. (2006) pp. 140-147
[18] G.Y. Zhou, J.H. Liu, W.J. Wang, G. Wen, Q.Y. Liu, "Study of the fatigue and wear characteristics of four wheel materials." *Journal of Modern Transportation*. 21[3] (2013) pp. 182-193.
[19] NTSB. *Rail Accident Brief RAB1712*. DCA15FR009. Washington, DC, USA (2016)
[20] TSB Canada. *Railway Investigations Report R14M0002*. Ottawa, ON, Canada (2025)
[21] S.S. Jafari, G.H. Majzoobi, E. Khademi, M. Kashfi. "Development of a new technique for measuring damage accumulation at high strain rates." *Engineering Fracture Mechanics*. 209. (2019) pp. 162-172.
[22] X. Gao, Y. Zhang, J. Peng. "NDE 4.0 in Railway Industry." *Handbook of Nondestructive Evaluation 4.0*. N. Meyendorf et.al., eds. Springer Nature Switzerland AG. (2025) pp. 1449-1468.
[23] T. Jendel. "Prediction of wheel profile wear—comparisons with field measurements." *Wear.* 253. (2002) pp. 89-99
[24] NTSB. *Railroad Investigation Report RIR-24-05*. RRD23MR005. Washington, DC, USA. (2024)